Dentomaxillofacial Radiology (2019) 48, 20180290

birpublications.org/dmfr

RESEARCH ARTICLE

Are metal artefact reduction algorithms effective to correct cone beam CT artefacts arising from the exomass?

[1]Amanda Pelegrin Candemil, [2]Benjamin Salmon, [1]Deborah Queiroz Freitas, [3]Glaucia Maria Bovi Ambrosano, [1]Francisco Haiter-Neto and [1]Matheus Lima Oliveira

[1]Department of Oral Diagnosis, Division of Oral Radiology, Piracicaba Dental School, University of Campinas, Piracicaba, Brazil; [2]Orofacial Pathologies, Imaging and Biotherapies Lab and Dental Medicine Department, Bretonneau Hospital, HUPNVS, AP-HP, Paris Descartes University - Sorbonne Paris Cité, Paris, France; [3]Department of Community Dentistry, Piracicaba Dental School, University of Campinas, Piracicaba, Brazil

The aim of this study was to evaluate the effectiveness of metal artefact reduction (MAR) in cone beam CT (CBCT) artefacts arising from metallic objects in the exomass. A radiographic phantom composed of 16 polypropylene tubes filled with a homogeneous radiopaque solution was created. CBCT scans were obtained with two units: Picasso Trio (Vatech, South Korea) and ProMax (Planmeca, Finland). The phantom was centred in a 5 × 5 cm field-of-view (FOV) with titanium and CoCr inserts in the exomass. All scans were repeated after enabling MAR. Mean voxel values were obtained from the 16 tubes and standard deviation was calculated as a way of measuring voxel value variability. Mean values and voxel value variability were compared individually in the presence and absence of MAR by means of analysis of variance, followed by Tukey's test ($\alpha = 0.05$). In the Picasso Trio, MAR significantly decreased mean voxel values ($p \leq 0.05$) and increased voxel value variability ($p > 0.05$) in the presence of titanium. When CoCr was present, no statistical difference ($p > 0.05$) was observed. In the ProMax, MAR increased significantly mean voxel values ($p \leq 0.05$) in the presence of titanium, and presented no significant difference ($p > 0.05$) for CoCr. Voxel value variability did not differ significantly ($p > 0.05$) for both materials. In conclusion, MAR was not effective to correct CBCT artefacts arising from metallic objects in the exomass in the two CBCT units used.
Dentomaxillofacial Radiology (2019) **48**, 20180290. doi: 10.1259/dmfr.20180290

Cite this article as: Candemil AP, Salmon B, Freitas DQ, Ambrosano GMB, Haiter-Neto F, Oliveira ML. Are metal artefact reduction algorithms effective to correct cone beam CT artefacts arising from the exomass?. *Dentomaxillofac Radiol* 2019; **48**: 20180290.

Keywords: cone-beam CT; dental implant; dental alloys; artifacts; *in vitro* techniques

Introduction

Cone beam CT (CBCT) is a well-accepted diagnostic tool in dental medicine that provides accurate three-dimensional images of dentomaxillofacial hard tissues.[1] A relevant limitation of this imaging modality is the presence of image artefact, which is a deviation between the reconstructed image and the real content of the studied object.[2] The most prominent source of artefact is beam hardening, which is accentuated in the presence of high-density structures of high atomic number, such as titanium implants, amalgam restorations and metallic prosthesis.[3,4]

Currently, the use of small field-of-view (FOV), also known as local tomography,[5] has been increasingly indicated because it enhances image quality and reduces X-radiation dose.[6] In this case, just a small portion of the object is imaged and the information from the exomass, *i.e.* structures that lie outside of the FOV but between the X-ray source and the image receptor, is dismissed to prevent negative interference; this is sometimes referred in the literature to

Correspondence to: Dr Matheus Lima Oliveira, E-mail: matheuso@unicamp.br
Received 07 August 2018; revised 30 November 2018; accepted 07 December 2018

as truncation correction. However, the presence of metallic objects in the exomass has demonstrated to produce unavoidable artefacts that results in inconsistent image reconstruction.[7,8]

Numerous methods and algorithms have been proposed to reduce CBCT artefacts.[9–12] One of them is metal artefact reduction (MAR) that has been widely assessed for different diagnostic tasks when metallic objects are observed inside the FOV.[13–17] Importantly, the wide use of small FOVs in dentistry, associated with the presence of metallic materials, which are not always within the FOV, has raised a very common clinical condition to be investigated. Therefore, the aim of this study was to evaluate the effectiveness of MAR in CBCT when metallic objects are present in the exomass.

Methods and materials

A radiographic phantom was custom-made to accurately simulate structures of the same physical density, homogeneously distributed in an FOV of 5 × 5 cm, according to previously published methodology.[8] A set of three titanium implants (KOPP, Curitiba, Brazil) and a set of three cylinders of cobalt-chromium (CoCr) alloy (Talmax, Curitiba, Brazil) with 15 mm of height and 5 mm of diameter were placed separately in the exomass to induce CBCT artefact formation. They were positioned vertically and arranged at the vertices of an imaginary isosceles triangle (right, left and anterior regions) at a distance of 15 mm from the most peripheral tubes (Figure 1). The physical density of the metallic materials was calculated based on the Archimedes principle on an analytical balance Discovery (OHAUS Corporation, Switzerland).[18] The phantom was filled with water to simulate the absorption and scattering of the X-rays in soft tissues.

CBCT scans were performed using two machines: Picasso Trio (Vatech, Seoul, South Korea) adjusted to 90 kVp, 3 mA, voxel size of 0.2 mm and exposure time of 24 s, and ProMax (Planmeca Oy, Helsinki, Finland) adjusted to 90 kVp, 3 mA, voxel size of 0.1 mm and exposure time of 12 s. The rotation arch and the number of basis images were, respectively, 360° and 720 for the Picasso Trio and 210° and 300 for the ProMax; importantly, these are not adjustable parameters. For each machine, ten repeated CBCT scans of the phantom were obtained with titanium or with CoCr alloy in the exomass. Subsequently, all scans were repeated with the use of MAR, totalling 80 CBCT scans. Figure 2 shows representative CBCT axial reconstruction of all experimental conditions. The ProMax CBCT unit presents three levels of MAR – low, medium and high – but, since no significant difference was observed between them,[16] this methodology made use of the medium level. Additionally, control images were obtained with ten repeated CBCT scans of the phantom without any metallic material in the exomass. The volumetric data were exported to DICOM file format and, in an endeavour to reduce possible negative interference on voxel values,[19] both CBCT units were warmed up with two initial acquisitions before the scans and a 10 min interval was respected between each scan.

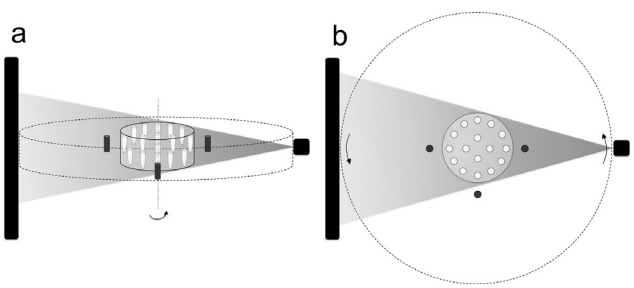

Figure 1 Geometric setting of the radiographic phantom in the CBCT unit: (a) lateral view; (b) axial view. The area between the full and dotted lines represents the exomass. The black rectangle and the shaded triangle represent, respectively, the image receptor and the X-ray beam. CBCT, cone beam CT.

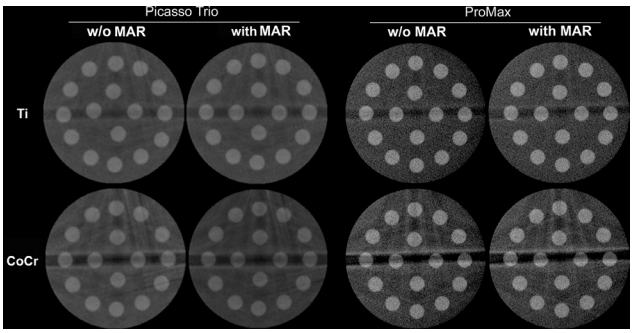

Figure 2 Representative axial reconstructions of the phantom with titanium implant (Ti) and cobalt–chrome (CoCr) in the exomass, without (w/o) and with MAR obtained with Picasso Trio and ProMax CBCT units. CBCT, cone beam CT; MAR, metal artefact reduction.

In the OsiriX MD DICOM viewer (Pixmeo SARL, Bernex, Switzerland), voxel values were obtained from 16 circular regions of interest of 8 mm^2 each in the most central axial reconstruction. Mean voxel value of each CBCT scan was calculated by averaging the 16 independent mean voxel values, and voxel value variability was obtained by calculating the standard deviation.

After the exploratory analysis, the data were submitted to analysis of variance in a factorial scheme 2 × 2 (MAR present/absent × metallic material) and Tukey's test with a level of significance of 5% ($\alpha = 0.05$).

Results

The use of MAR significantly reduced ($p \leq 0.05$) the mean voxel value when titanium implants were in the exomass in the Picasso Trio unit. Conversely, under the same conditions in the ProMax unit, the mean

Table 1 Mean voxel values (standard deviation) in function of the metal artefact reduction (MAR) algorithm, dental material in the exomass and CBCT unit

CBCT unit	*Material*	*w/o MAR*	*with MAR*
Picasso Trio	Titanium	815.13 (4.28)[a,b,c,d]	791.31 (6.21)[a,d]
	CoCr	729.01 (10.83)[d]	714.09 (2.72)[d]
ProMax	Titanium	804.20 (16.87)[a,d]	823.51 (12.46)[c,d]
	CoCr	688.09 (19.25)[d]	688.51 (12.20)[d]

CBCT, cone beam CT; MAR, metal artefact reduction.
[a]Titanium significantly higher ($p \leq 0.05$) than CoCr for the same CBCT unit.
[b]w/o MAR significantly higher ($p \leq 0.05$) than with MAR for titanium in the Picasso Trio.
[c]with MAR significantly higher ($p \leq 0.05$) than w/o MAR for titanium in the ProMax.
[d]Significantly lower ($p \leq 0.05$) than control images (Picasso Trio = 882.13 (4.99); ProMax = 845.08 (4.24)).

voxel value increased significantly ($p \leq 0.05$). In both CBCT units, when CoCr objects were in the exomass, no significant difference ($p > 0.05$) was observed in the mean voxel value with or without MAR. The presence of titanium implants in the exomass significantly increased ($p \leq 0.05$) mean voxel value compared to the presence of CoCr objects, under all conditions. Control images presented significantly higher mean voxel values than those with metallic materials in the exomass (Table 1).

Regarding voxel value variability, in the Picasso Trio, the use of MAR significantly increased ($p \leq 0.05$) the values in the presence of titanium implants in the exomass. For the same CBCT unit, when CoCr objects were in the exomass, no significant difference ($p > 0.05$) was observed in the voxel value variability with or without MAR. Similarly, in the ProMax unit, the use of MAR did not result in significant difference ($p > 0.05$) in voxel value variability for both materials. Under all conditions, CoCr objects led to significantly higher ($p \leq 0.05$) voxel value variability than titanium implants. Control images presented significantly lower voxel value variability than those with metallic materials in the exomass, except for the ProMax unit in the presence of titanium implants (Table 2).

Table 2 Voxel value variability (standard deviation) in function of the metal artefact reduction (MAR) algorithm, dental material in the exomass and CBCT unit

CBCT unit	*Material*	*w/o MAR*	*with MAR*
Picasso Trio	Titanium	84.27 (2.71)[c]	93.41 (2.17)[a,c]
	CoCr	158.04 (2.62)[b,c]	155.77 (3.18)[b,c]
ProMax	Titanium	76.10 (6.42)	72.13 (4.01)
	CoCr	177.02 (8.24)[b,c]	174.94 (6.15)[b,c]

CBCT, cone beam CT; MAR, metal artefact reduction.
[a]with MAR significantly higher ($p \leq 0.05$) than w/o MAR for titanium in the Picasso Trio.
[b]CoCr significantly higher ($p \leq 0.05$) than titanium for both CBCT units.
[c]Significantly higher ($p \leq 0.05$) than control images (Picasso Trio = 53.193 (2.01); ProMax = 72.09 (1.82)).

Discussion

Recent studies have demonstrated that CBCT image quality is influenced by parameters such as kilovoltage peak,[4] milliamperage[20,21] and voxel and FOV sizes.[6,22,23] Consequently, diverse combinations of these parameters affect differently the final image. Moreover, it is well known that CBCT image is severely influenced by artefacts, which compromise specific diagnostic tasks.[24–26] Thus, in an endeavour to overcome some artefact-related limitations, MAR algorithms have been developed and, given its relatively recent advent, scientific studies have focused on the effectiveness of MAR when high-density objects of high atomic number are observed inside the FOV.

The increased indication of small FOV CBCT in dental medicine has posed a challenge for MAR algorithms in clinical conditions in which the source of artefact is not inside the FOV but between the source of X-rays and the image receptor. In the present study, for both CBCT units tested, the MAR algorithm was not effective in improving image quality by reducing voxel value variability in the presence of metallic materials in the exomass. Similarly, other studies having metallic materials inside the FOV indicated that MAR was not effective for the reduction of the artefact appearance[3,27] and for the detection of root fracture,[28,29] peri-implant defects[30,31] and furcal perforations.[32] Conversely, others studies showed that the MAR is an effective algorithm for the improvement of subjective image quality,[33] detection of caries[13] and reduction of the voxel value variability.[4,34–36] Importantly, none of these studies included metallic materials in the exomass.

Considering that CBCT artefacts do not affect the FOV homogeneously,[3] in this study, mean voxel values were obtained from ROIs covering the whole axial reconstruction. In addition, studies have shown that the MAR algorithm is more effective when the object is centred in the FOV.[14,34] However, in the present research, no metallic object was intentionally placed inside the FOV, only in the exomass.

The use of the MAR algorithm in the presence of titanium implants in the exomass decreased mean voxel value in the Picasso Trio and increased mean voxel value in the ProMax. As both CBCT units could not be adjusted at exact the same exposure parameters, no direct comparison was intended to be made between them. Instead, statistical analyses compared CBCT scans with and without MAR, which indicates that these divergent results can be attributed to the MAR algorithm of each individual machine. Also, MAR algorithms do not alter exposure parameters; it only increases the reconstruction time and file size,[36] which reinforces the hypothesis that MAR algorithms do not work the same way between CBCT units. When the exomass was composed of cylinders made of

CoCr alloy, the MAR algorithm did not promote any significant change in mean voxel value.

The presence of high-density materials in CBCT causes scatter and beam-hardening artefacts,[3,32] which are directly proportional to voxel value variability; increased values of variability represent a greater impact of artefacts on the CBCT image, and a consequent reduction in image quality.[37] The present study demonstrated that voxel value variability does not change when the MAR algorithm is activated, with the exception of the Picasso Trio unit for titanium implants, which showed significantly increased values. This is the opposite of what one would expect when MAR is activated and could possibly reveal that MAR is not able to recognize an artefact whose source is in the exomass. Interestingly, in the study of Bezerra et al MAR reduced contrast-to-noise ratio when the artefact source was inside the FOV.[29]

As expected, when comparing the materials in the exomass, CoCr alloy showed lower mean voxel value and higher voxel value variability regardless of the MAR activation, in Picasso Trio and ProMax units. The physical properties – atomic number and physical density – of the objects used in this study (titanium: 22 and 4.301 kg m^{-3}; cobalt: 27, chrome: 24 and CoCr: 8.8 kg m^{-3}, respectively) confirms that higher values lead to more impacting results.

Limited information is released about the real action of MAR algorithms, which makes it difficult to interpret some conflicting results observed in the scientific literature. Despite this, Wang et al stated that MAR can be a pre- or post-processing algorithm[38]; and the former has shown a greater efficiency than the latter.[35,39] According to Schulze et al, post-processing algorithms do not correct missed data, which results in an estimated correction.[40] In the ProMax CBCT unit, the MAR algorithm is power-based on a selected threshold and all voxels with higher density are corrected, reducing artefacts.[31] However, no further information was obtained related to the processing method. For the Picasso Trio, no information on the operation of the MAR algorithm is disclosed. Nevertheless, Queiroz et al observed that MAR is applied after automatic thresholding of raw images in the voxel values corrupted by artefacts, followed by image correction, which suggests this is a post-processing algorithm.[14]

Any algorithm that effectively and accurately reduces CBCT artefact without increasing radiation dose is highly beneficial for the patient as it would positively influence image quality and allow for better diagnosis. Technological development should also focus on reducing CBCT artefacts arising from metallic materials in the exomass.

Conclusion

The metal artefact reduction algorithm is not effective to reduce CBCT voxel value variability when artefacts arise from the exomass in the two CBCT units used. Furthermore, metal artefact reduction affects mean voxel values differently depending on the composition of the artefact source and on the CBCT machine. Limited information is available on the principles of this algorithm.

Acknowledgment

The authors gratefully acknowledge financial support from Coordenação de Aperfeiçoamento de Pessoal de Nível Superior - Brasil (CAPES) – Finance code 001, and from the International Relations Office (DERI 26/2016) at UNICAMP. The authors deny any conflicts of interest related to this study.

References

1. Abramovitch K, Rice DD. Basic Principles of Cone Beam Computed Tomography. *Dent Clin North Am* 2014; **58**: 463–84. doi: https://doi.org/10.1016/j.cden.2014.03.002
2. Makins SR. Artifacts interfering with interpretation of cone beam computed tomography images. *Dent Clin North Am* 2014; **58**: 485–95. doi: https://doi.org/10.1016/j.cden.2014.04.007
3. Parsa A, Ibrahim N, Hassam B, Van Der Stelt P, Wismeijer D. Influence of object location in Cone Beam Computed Tomography (NewTom 5G and 3G Accuitomo 170) on grey value measurements at an implant site. *Oral radiology* 2014; **30**: 153–9.
4. Helvacioglu-Yigit D, Demirturk Kocasarac H, Bechara B, Noujeim M. Evaluation and Reduction of Artifacts Generated by 4 Different Root-end Filling Materials by Using Multiple Cone-beam Computed Tomography Imaging Settings. *J Endod* 2016; **42**: 307–14. doi: https://doi.org/10.1016/j.joen.2015.11.002
5. Siltanen S, Kolehmainen V, Järvenpää S, Kaipio JP, Koistinen P, Lassas M, et al. Statistical inversion for medical x-ray tomography with few radiographs: I. General theory. *Phys Med Biol* 2003; **48**: 1437–63. doi: https://doi.org/10.1088/0031-9155/48/10/314
6. Pauwels R, Jacobs R, Bogaerts R, Bosmans H, Panmekiate S. Reduction of scatter-induced image noise in cone beam computed tomography: effect of field of view size and position. *Oral Surg Oral Med Oral Pathol Oral Radiol* 2016; **121**: 188–95. doi: https://doi.org/10.1016/j.oooo.2015.10.017
7. Meilinger M, Schmidgunst C, Schütz O, Lang EW. Metal artifact reduction in cone beam computed tomography using forward projected reconstruction information. *Zeitschrift für Medizinische Physik* 2011; **21**: 174–82. doi: https://doi.org/10.1016/j.zemedi.2011.03.002
8. Candemil AP, Salmon B, Freitas DQ, Ambrosano GM, Haiter-Neto F, Oliveira ML. Metallic materials in the exomass impair cone beam CT voxel values. *Dentomaxillofac Radiol* 2018; **47**: 20180011: 20180011: . doi: https://doi.org/10.1259/dmfr.20180011
9. Wang Q, Li L, Zhang L, Chen Z, Xing Y, Kang K. Reducing Metal Artifacts by Pre-Processing Projection Data in Dental CBCT with a Half-size Detector. *IEEE Nuclear Science Symposium Conference Record* 2011;: 3434–7.
10. Zhang Z, Han X, Pearson E, Pelizzari C, Sidky EY, Pan X. Artifact reduction in short-scan CBCT by use of optimization-based reconstruction. *Phys Med Biol* 2016; **61**: 3387–406. doi: https://doi.org/10.1088/0031-9155/61/9/3387

11. Xia D, Langan DA, Solomon SB, Zhang Z, Chen B, Lai H, et al. Optimization-based image reconstruction with artifact reduction in C-arm CBCT. *Phys Med Biol* 2016; **61**: 7300–33. doi: https://doi.org/10.1088/0031-9155/61/20/7300
12. Dang H, Stayman JW, Sisniega A, Zbijewski W, Xu J, Wang X, et al. Multi-resolution statistical image reconstruction for mitigation of truncation effects: application to cone-beam CT of the head. *Phys Med Biol* 2017; **62**: 539–59. doi: https://doi.org/10.1088/1361-6560/aa52b8
13. Cebe F, Aktan AM, Ozsevik AS, Ciftci ME, Surmelioglu HD. The effects of different restorative materials on the detection of approximal caries in cone-beam computed tomography scans with and without metal artifact reduction mode. *Oral Surg Oral Med Oral Pathol Oral Radiol* 2017; **123**: 392–400. doi: https://doi.org/10.1016/j.oooo.2016.11.008
14. Queiroz PM, Santaella GM, da Paz TD, Freitas DQ. Evaluation of a metal artefact reduction tool on different positions of a metal object in the FOV. *Dentomaxillofac Radiol* 2017; **46**: 20160366. doi: https://doi.org/10.1259/dmfr.20160366
15. Queiroz PM, Oliveira ML, Groppo FC, Haiter-Neto F, Freitas DQ. Evaluation of metal artefact reduction in cone-beam computed tomography images of different dental materials. *Clinical Oral Investigations* 2018; **22**: 419–23. doi: https://doi.org/10.1007/s00784-017-2128-9
16. Freitas DQ, Fontenele RC, Nascimento EHL, Vasconcelos TV, Noujeim M. Influence of acquisition parameters on the magnitude of cone beam computed tomography artifacts. *Dentomaxillofac Radiol* 2018; **47**: 20180151: 20180151: . doi: https://doi.org/10.1259/dmfr.20180151
17. Fox A, Basrani B, Lam EWN. The Performance of a Zirconium-based Root Filling Material with Artifact Reduction Properties in the Detection of Artificially Induced Root Fractures Using Cone-beam Computed Tomographic Imaging. *J Endod* 2018; **44**: 828–33. doi: https://doi.org/10.1016/j.joen.2018.02.007
18. Scarfe WC, Farman AG, Sukovic P. Clinical applications of conebeam computed tomography in dental practice. *J Can Dent Assoc* 2006; **72**: 75–80.
19. Spin-Neto R, Gotfredsen E, Wenzel A. Variation in voxel value distribution and effect of time between exposures in six CBCT units. *Dentomaxillofacial Radiology* 2014; **43**: 20130376. doi: https://doi.org/10.1259/dmfr.20130376
20. Pauwels R, Jacobs R, Singer SR, Mupparapu M. CBCT-based bone quality assessment: are Hounsfield units applicable? *Dentomaxillofac Radiol* 2015; **44**: 20140238. doi: https://doi.org/10.1259/dmfr.20140238
21. Oliveira ML, Freitas DQ, Ambrosano GM, Haiter-Neto F. Influence of exposure factors on the variability of CBCT voxel values: a phantom study. *Dentomaxillofac Radiol* 2014; **43**: 20140128: 20140128: . doi: https://doi.org/10.1259/dmfr.20140128
22. Spin-Neto R, Gotfredsen E, Wenzel A. Variation in voxel value distribution and effect of time between exposures in six CBCT units. *Dentomaxillofac Radiol* 2014; **43**: 20130376. doi: https://doi.org/10.1259/dmfr.20130376
23. Iikubo M, Nishioka T, Okura S, Kobayashi K, Sano T, Katsumata A, et al. Influence of voxel size and scan field of view on fracture-like artifacts from gutta-percha obturated endodontically treated teeth on cone-beam computed tomography images. *Oral Surg Oral Med Oral Pathol Oral Radiol* 2016; **122**: 631–7. doi: https://doi.org/10.1016/j.oooo.2016.07.014
24. Iikubo M, Osano T, Sano T, Katsumata A, Ariji E, Kobayashi K, et al. Root canal filling materials spread pattern mimicking root fractures in dental CBCT images. *Oral Surg Oral Med Oral Pathol Oral Radiol* 2015; **120**: 521–7. doi: https://doi.org/10.1016/j.oooo.2015.06.030
25. Chang E, Lam E, Shah P, Azarpazhooh A. Cone-beam computed tomography for detecting vertical root fractures in endodontically treated teeth: a systematic review. *J Endod* 2016; **42**: 177–85. doi: https://doi.org/10.1016/j.joen.2015.10.005
26. Gaalaas L, Tyndall D, Mol A, Everett ET, Bangdiwala A. Ex vivo evaluation of new 2D and 3D dental radiographic technology for detecting caries. *Dentomaxillofac Radiol* 2016; **45**: 20150281. doi: https://doi.org/10.1259/dmfr.20150281
27. Vasconcelos KF, Nicolielo LF, Nascimento MC, Haiter-Neto F, Bóscolo FN, Van Dessel J, et al. Artefact expression associated with several cone-beam computed tomographic machines when imaging root filled teeth. *Int Endod J* 2015; **48**: 994–1000. doi: https://doi.org/10.1111/iej.12395
28. Bechara B, Alex McMahan C, Moore WS, Noujeim M, Teixeira FB, Geha H. Cone beam CT scans with and without artefact reduction in root fracture detection of endodontically treated teeth. *Dentomaxillofac Radiol* 2013; **42**: 20120245. doi: https://doi.org/10.1259/dmfr.20120245
29. Bezerra IS, Neves FS, Vasconcelos TV, Ambrosano GM, Freitas DQ. Influence of the artefact reduction algorithm of Picasso Trio CBCT system on the diagnosis of vertical root fractures in teeth with metal posts. *Dentomaxillofac Radiol* 2015; **44**: 20140428. doi: https://doi.org/10.1259/dmfr.20140428
30. Kamburoğlu K, Kolsuz E, Murat S, Eren H, Yüksel S, Paksoy CS. Assessment of buccal marginal alveolar peri-implant and periodontal defects using a cone beam CT system with and without the application of metal artefact reduction mode. *Dentomaxillofac Radiol* 2013; **42**: 20130176: 20130176: . doi: https://doi.org/10.1259/dmfr.20130176
31. de-Azevedo-Vaz SL, Peyneau PD, Ramirez-Sotelo LR, Vasconcelos KF, Campos PS, Haiter-Neto F. Efficacy of a cone beam computed tomography metal artifact reduction algorithm for the detection of peri-implant fenestrations and dehiscences. *Oral Surg Oral Med Oral Pathol Oral Radiol* 2016; **121**: 550–6. doi: https://doi.org/10.1016/j.oooo.2016.01.013
32. Kamburoğlu K, Yılmaz F, Yeta EN, Özen D. Assessment of furcal perforations in the vicinity of different root canal sealers using a cone beam computed tomography system with and without the application of artifact reduction mode: an ex vivo investigation on extracted human teeth. *Oral Surg Oral Med Oral Pathol Oral Radiol* 2016; **121**: 657–65. doi: https://doi.org/10.1016/j.oooo.2016.01.010
33. Enomoto Y, Yamauchi K, Asano T, Otani K, Iwama T. Effect of metal artifact reduction software on image quality of C-arm cone-beam computed tomography during intracranial aneurysm treatment. *Interv Neuroradiol* 2018; **24**: 303–8. doi: https://doi.org/10.1177/1591019917754039
34. Bechara BB, Moore WS, McMahan CA, Noujeim M. Metal artefact reduction with cone beam CT: an in vitro study. *Dentomaxillofac Radiol* 2012; **41**: 248–53. doi: https://doi.org/10.1259/dmfr/80899839
35. Bechara B, McMahan CA, Geha H, Noujeim M. Evaluation of a cone beam CT artefact reduction algorithm. *Dentomaxillofac Radiol* 2012; **41**: 422–8. doi: https://doi.org/10.1259/dmfr/43691321
36. Vasconcelos TV, Bechara BB, McMahan CA, Freitas DQ, Noujeim M. Evaluation of artifacts generated by zirconium implants in cone-beam computed tomography images. *Oral Surg Oral Med Oral Pathol Oral Radiol* 2017; **123**: 265–72. doi: https://doi.org/10.1016/j.oooo.2016.10.021
37. Pauwels R, Stamatakis H, Bosmans H, Bogaerts R, Jacobs R, Horner K, et al. SEDENTEXCT Project Consortium. Quantification of metal artifacts on cone beam computed tomography images. *Clin Oral Implants Res* 2013; **24**: 94–9.
38. Wang Q, Li L, Zhang L, Chen Z, Kang K. A novel metal artifact reducing method for cone-beam CT based on three approximately orthogonal projections. *Phys Med Biol* 2013; **58**: 1–17. doi: https://doi.org/10.1088/0031-9155/58/1/1
39. Mahnken AH, Raupach R, Wildberger JE, Jung B, Heussen N, Flohr TG, et al. A new algorithm for metal artifact reduction in computed tomography: in vitro and in vivo evaluation after total hip replacement. *Invest Radiol* 2003; **38**: 769–75.
40. Schulze RK, Berndt D, d'Hoedt B. On cone-beam computed tomography artifacts induced by titanium implants. *Clin Oral Implants Res* 2010; **21**: 100–7. doi: https://doi.org/10.1111/j.1600-0501.2009.01817.x